A98-31519 ICAS-98-2,8,1

STABILITY ANALYSIS BY THE OS AND PSE APPROACHES: COMPARISONS WITH EXPERIMENTS

Marc Langlois*
Bombardier Aerospace Group, Dorval (Québec), Canada

Patric MacDonald†
École Polytechnique de Montréal, Montréal (Québec), Canada

Christian Masson‡
École de technologie supérieure, Montréal (Québec), Canada

Grégoire Casalis§
ONERA-CERT, Toulouse, France

Ion Paraschivoiu¶
École Polytechnique de Montréal, Montréal (Québec), Canada

Abstract

The objective of the work described in this article is to conduct a detailed comparison of parallel and non-parallel stability results with experimental measurements. To this end, two stability analysers are used: the first one is based on the linear, three-dimensional, parallel stability equations (Orr-Sommerfeld problem) while the second one solves the incompressible Parabolised Stability Equations (PSE). The PSE formulation takes into account the variations of the mean flow and disturbance quantities in the principal direction of the flow (typically the chordwise direction) which are neglected in the parallel approach. In the PSE approach, the amplitude of a perturbation can be related to a "physically measurable" quantity, a possibility that does not exist with the parallel stability theory. It is therefore expected that the PSE results may provide a better reproduction of some experimentally-observed features than has so far been obtained using the parallel theory. In this article, fluctuation spectra obtained by the OS and PSE approaches on the ONERA D and AFVD 82 swept wings are compared to hot-wire and hot-film experimental data. On the AFVD 82 wing, the theoretical spectra predicted by the PSE approach are indeed in much better agreement with the experimental data than those obtained with the parallel formulation. In the case of the ONERA D wing, the improvement in accuracy obtained by using the PSE approach instead of the parallel formulation is much less significant.

*Staff Engineer, Advanced Aerodynamics. AIAA Member
†M.A.Sc. Student, AIAA Member
‡Associate Professor, Mech. Eng. Dept., AIAA Member
§Research Engineer, DMAE
¶Aeronautical Chair Professor, AIAA Associate Fellow

1 Introduction

The prediction of the location of transition from a laminar flow to a turbulent one plays a fundamental role in the analysis of the flowfield around most configurations of engineering interest. The linear stability theory, in its "classical", Orr-Sommerfeld (OS) form, has been extensively used for that purpose. A comprehensive review of the capabilites and limitations of this theory is provided by Reed et al.[1]. One of its main assumptions is that the boundary layer can be considered as locally-parallel, i.e. the mean flow variations in x and z, the coordinates in the plane of the surface along which the boundary layer grows, are neglected in the stability analysis. The influence of this hypothesis has been studied for a number of years with different methods[2,3], based mostly on the multiple-scale approach. In most cases, though, the studies were limited to the two-dimensional flat-plate flow for which the non-parallel effects are indeed small.

The Parabolised Stability Equations (PSE) approach was developed more recently by Herbert and Bertolotti[4] and the group of Dallmann at DLR-Göttingen[5]. It takes into account the dominant non-parallel effects in the mean flow, as well as in the perturbed quantities and can easily be applied to more complex flows, such as that about a swept wing, for which the non-parallel effects are not known a priori. The numerical solution of the PSE is carried within a space-marching procedure, with the parallel approximation and the first-order non-parallel correction solved simultaneously. This contrasts with the classical multiple-scale non-parallel approaches[2,3,6,7] which result in a sequential resolution of the problem.

After developing a three-dimensional, compressible stability analyser based on the parallel theory[8,9], the research group of the J.-A. Bombardier Aeronautical Chair has recently developed a computer code

21st ICAS Congress
13-18 September 1998
Melbourne, Australia

based on this PSE approach, with the collaboration of ONERA-CERT[10,11]. This computer code was used to study the importance of non-parallel effects on different wings. That study revealed that the inclusion of the non-parallel effects in the stability analysis could result in a shift of the dominant instability from a streamwise to a crossflow one, accompanied by a decrease of the critical frequency. This behaviour was linked to the presence of two maxima in the fluctuation spectrum, a feature that has been observed experimentally[12] but that the parallel stability equations seem to be unable to reproduce. A comparison of experimental and non-parallel theoretical fluctuation spectra[13] was also conducted recently. It showed that the non-uniqueness in the definition of the fluctuation growth rate inherent to the PSE approach could actually be exploited to better reproduce the experimental data by considering the proper "physical quantity" in this definition.

Following a description of the mathematical formulation and its numerical implementation, this paper will continue the previous investigation by detailed comparisons of the experimental fluctuation spectra obtained at ONERA by Arnal and Juillen[12] with those calculated using both the parallel and the PSE approaches.

2 Mathematical Formulation

The description of the mathematical models will concentrate on the non-parallel Parabolised Stability Equations (PSE). The differences between this approach and the classical parallel linear stability theory (Orr-Sommerfeld theory) will be pointed out when appropriate.

2.1 Parabolised Stability Equations

In the present work, the linear PSE approach was implemented for an incompressible flow over an infinite swept wing (three-dimensional flow). A primitive-variables formulation, as described by Casalis[14], was used. Fig. 1 shows the coordinate system considered in the development of the PSE model: x and z are along the wing surface, respectively in the chordwise and spanwise directions, and y is normal to the surface. The velocity components in the x, y and z directions are U, V and W, respectively.

As in the classical Orr-Sommerfeld (OS) linear stability theory, the PSE approach to stability analysis is based on the decomposition of flow variables (for an incompressible flow, the velocity components u, v and w and the pressure p) into a mean, steady part and a quasi-sinusoidal perturbation. The main difference between the OS and PSE approaches is in the form assumed for the mean flow and the perturbations. Specifically, the flow decomposition in the PSE

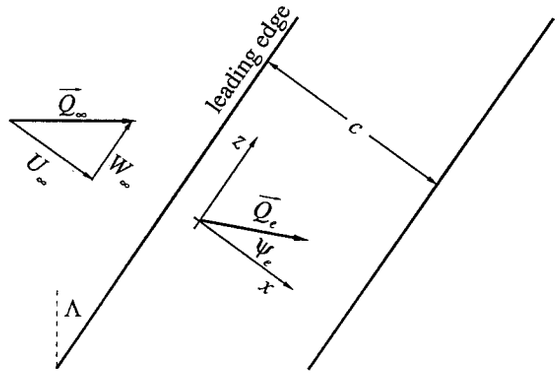

Figure 1: Coordinate system

formulation is given by:

$$\begin{bmatrix} u \\ v \\ w \\ p \end{bmatrix} = \begin{bmatrix} U(x,y) \\ V(y) \\ W(x,y) \\ P(x) \end{bmatrix} + \begin{bmatrix} \tilde{u}(x,y,z,t) \\ \tilde{v}(x,y,z,t) \\ \tilde{w}(x,y,z,t) \\ \tilde{p}(x,y,z,t) \end{bmatrix} \quad (1)$$

$$\begin{bmatrix} \tilde{u} \\ \tilde{v} \\ \tilde{w} \\ \tilde{p} \end{bmatrix} = \begin{bmatrix} \hat{u}(x,y) \\ \hat{v}(x,y) \\ \hat{w}(x,y) \\ \hat{p}(x,y) \end{bmatrix} e^{i\left(\int_{x_0}^{x} \alpha(\xi)\, d\xi + \beta z - \omega t\right)} \quad (2)$$

Equation (1) shows that the x-derivatives of the mean flow and its normal component, V, are no longer assumed to be negligible. The amplitude functions are now seen to depend on y and x whereas they depend only on y in the OS formulation, and the wavenumber α, locally constant in the OS theory, also depends on x. This x-dependence of the mean flow and amplitude functions is assumed to be much weaker than their y-dependence, thus allowing some terms to be dropped based on a scale analysis. These neglected terms correspond essentially to the 2nd-order terms of the multiple-scale approaches.

The system of equations for the linear PSE is obtained from the *full* Navier-Stokes equations by substituting the above expressions, subtracting the mean flow solution, neglecting derivatives of order 2 and higher in x and, according to the linear stability analysis, eliminating terms that are quadratic in the perturbations. Neglecting the curvature terms related to the curvilinear nature of the chosen (x, y, z) coordinate system, a system of equations of the following form is obtained:

$$(L_{OS} + L_{NP})\hat{q} + N\frac{\partial \hat{q}}{\partial x} = 0 \quad (3)$$

where L_{OS}, L_{NP} and N are operators in y with coefficients that depend on x and y through the mean flow profiles, and $\hat{q}$ is the vector of unknown amplitude functions, $\hat{q} = [\hat{u}, \hat{v}, \hat{w}, \hat{p}]^T$. L_{OS} is the same operator that appears in the parallel formulation ($L_{OS}\hat{q} = 0$), while L_{NP} contains non-parallel terms linked to the mean flow and the term $d\alpha/dx$.

It should be noted that, in order to effectively obtain a parabolic system of equations with the primitive-variables formulation, the term $\partial\hat{p}/\partial x$ has been neglected in the x-momentum equation. Airiau[15] has verified numerically that this term is indeed negligible ($|\partial\hat{p}/\partial x| \ll |i\alpha\hat{p}|$).

The boundary conditions that apply to this system are the usual ones of adherence to the surface and damping of the perturbations away from the surface:

$$\begin{array}{lll} \hat{u}(x,0) = 0 & \hat{v}(x,0) = 0 & \hat{w}(x,0) = 0 \\ \lim_{y\to\infty} \hat{u} = 0 & \lim_{y\to\infty} \hat{v} = 0 & \lim_{y\to\infty} \hat{w} = 0 \end{array} \quad (4)$$

The spatial stability formulation is used (ω real, α and β complex). In the present PSE approach, on an infinite swept wing, there is no amplification in the z-direction ($\beta_i = 0, \beta = \beta_r$) and the spanwise dimensional wavenumber β^* is assumed to be constant.

2.2 Amplitudes

The solution of the parallel (OS) stability equations yields a uniquely-defined spatial amplification rate, $\sigma = -\alpha_i$. In the PSE, as in other non-parallel stability theories, it is possible to consider different "physical" amplitudes of the perturbation, based on various "measurable" properties of the disturbance vector. This feature is most useful when conducting comparisons with experimental results, as it allows to select the amplitude that corresponds to the quantity that is actually measured. For instance, the following amplitudes would be used to compare with hot-wire, hot-film and pressure-tap measurements, respectively:

$$\begin{aligned} \hat{A}_{u_y}(x) &= |\hat{u}(x,y)|_{y=y_0} \\ \hat{A}_\tau(x) &= \left|\frac{\partial\hat{u}(x,y)}{\partial y}\right|_{y=0} \\ \hat{A}_p(x) &= |\hat{p}(x,y)|_{y=0} \end{aligned} \quad (5)$$

For transition prediction, on the other hand, the amplitudes most commonly used are based on the maximum values of the perturbation x and z velocity components and the integrated fluctuation energy:

$$\begin{aligned} \hat{A}_u(x) &= \max_y |\hat{u}(x,y)| \\ \hat{A}_w(x) &= \max_y |\hat{w}(x,y)| \\ \hat{A}_e(x) &= \sqrt{\int_0^\infty (|\hat{u}|^2 + |\hat{v}|^2 + |\hat{w}|^2)\, dy} \end{aligned} \quad (6)$$

To each of these amplitudes corresponds a spatial growth rate, given by

$$\sigma_m = -\alpha_i + \frac{1}{\hat{A}_m}\frac{d\hat{A}_m}{dx} \quad (7)$$

as well as a wavenumber and wave orientation.

2.3 Transition Prediction

The e^n empirical method is used to relate the calculated growth rates to the location of transition. In the classical parallel approach, different integration strategies arise from the fact that, with the dimensional frequency f fixed, there still remains the wavenumber β^* to be determined[16]. With the PSE hypotheses, however, only the constant-β^* method is appropriate:

$$n_m(\mathrm{f}, x) = \max_{\beta^*}\left\{\int_{x_0}^{x} \sigma_m(\mathrm{f}, \beta^*, \xi)\, d\xi\right\} \quad (8)$$

The same definition for the n factor also applies to the parallel theory, though it is then of course uniquely defined, as the amplification rate.

2.4 Normalisation

In Eq. (1), the x-dependence of the perturbation is split between the amplitude functions and the exponential term containing $\alpha(x)$. To lift this ambiguity and determine α uniquely, Herbert[4] proposed the use of a normalisation relation, imposing the slow variation in x of the amplitude functions ($\partial\hat{q}/\partial x \ll i\alpha\hat{q}$). The normalisation relation adopted consists in imposing $\hat{A}_e$=cte., which results in the following:

$$N_e(x) = \int_0^\infty \left(\bar{u}\frac{\partial\hat{u}}{\partial x} + \bar{v}\frac{\partial\hat{v}}{\partial x} + \bar{w}\frac{\partial\hat{w}}{\partial x}\right) dy = 0 \quad (9)$$

where $\bar{q}$ designates the complex conjugate of $\hat{q}$.

3 Numerical Implementation

3.1 Discretisation

The x-derivatives in Eq. (3) are evaluated using first-order upwind differencing:

$$\left.\frac{\partial\hat{\phi}}{\partial x}\right|_j^k = \frac{\hat{\phi}_j^k - \hat{\phi}_{j-1}^k}{x_j - x_{j-1}} \quad (10)$$

where j and k are the grid indices in x and y, respectively. With this discretisation, and the introduction of the y-derivatives of $\hat{u}$ and $\hat{w}$ as new dependent variables, the system given by Eq. (3) is transformed into the following first-order semi-discrete system:

$$\left.\frac{\partial\hat{\phi}}{\partial y}\right|_j^k = M_{1j}^k\hat{\phi}_j^k + M_{2j}^k \quad (11)$$

in which

$$\hat{\phi} = \left[\hat{u}, \hat{v}, \hat{w}, \hat{p}, \frac{\partial \hat{u}}{\partial y}, \frac{\partial \hat{w}}{\partial y}\right]^T \tag{12}$$

and M_{2j}^k contains terms related to $\hat{\phi}_{j-1}^k$. Hirsch's fourth-order compact scheme[17] is used to express the y-derivatives. After rearrangement of the equations, a block tridigonal system of equations is obtained:

$$N_1^k \hat{\phi}^{k+1} + N_2^k \hat{\phi}^k + N_3^k \hat{\phi}^{k-1} = P^k \tag{13}$$

which can be solved by a LU decomposition method.

3.2 Initial Conditions

The system of equations to be solved being parabolic in x, initial values of α and $\hat{q}$ are required to start the calculations. In our approach, these are provided by a local parallel (OS) solution, thereby inducing a transient phase in the first few stations in x. In order to minimise the influence of this phase, it is important to initialise the calculations sufficiently but not too far upstream of the (a priori unknown) non-parallel neutral curve. The sensitivity of the PSE results to the initial OS solution has been illustrated by Langlois et al.[10]. It might be possible to overcome this difficulty by using a non-parallel local solution, as proposed by Masson et al.[7], to start the PSE.

3.3 Calculation Procedure

The parallel stability problem leads to a local eigenvalue problem, which can be solved by a number of numerical techniques. The Parabolised Stability Equations, on the other hand, are more akin to the boundary layer equations and must be solved using a space-marching procedure in x. At each x-station, an iterative procedure is used to solve Eq. (13) subject to the normalisation (9). This is illustrated by the algorithm presented in Fig. 2. An initial guess of α, $\alpha_j^{(1)}$, is obtained either from the initial conditions (at $j = j_0$) or from the value of α at previous stations. With $\alpha_j^{(p)}$ fixed, the solution of Eq. (13) yields new values of the amplitude functions, $\hat{q}_j^{(p+1)}$. The norm is then calculated and used to define a new estimate of α:

$$\alpha_j^{(p+1)} = \alpha_j^{(p)} - i\frac{N_e(\hat{q}_j^{(p+1)})}{\hat{A}_e^2(\hat{q}_j^{(p+1)})} \tag{14}$$

The procedure is repeated until convergence of α_j, which implies naturally $N_e = 0$, and the calculations then proceed to the next station in x.

4 Results

The influence of non-parallel effects on transition prediction was illustrated in Ref. (11) by correlating the

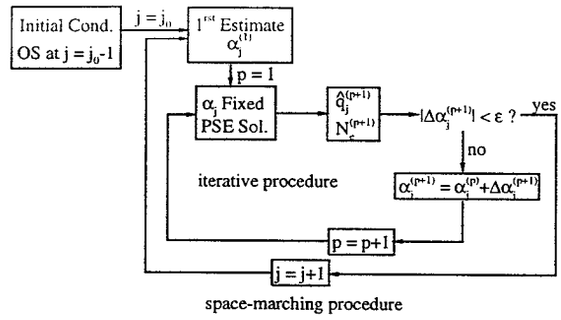

Figure 2: PSE Algorithm

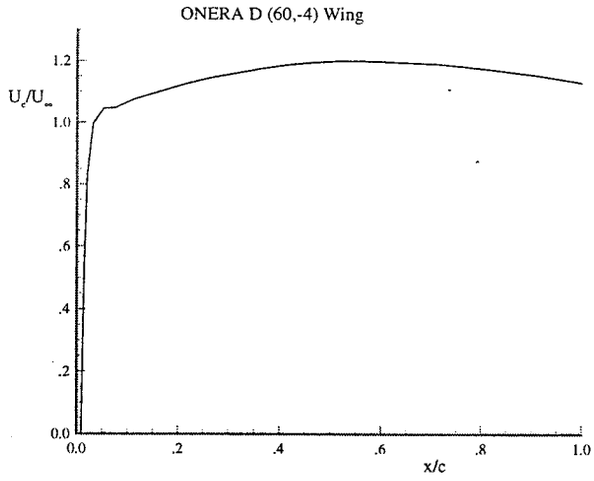

Figure 3: ONERA D (60,-4) — External velocity distribution

n factors calculated using the OS and PSE approaches with the location of transition measured by Arnal and Juillen[12]. This was done for two different infinite swept wings, one with the ONERA D airfoil (sweep angle of 60°, incidence of -4°) and the other with the AFVD 82 airfoil (sweep angle of 49°, incidence of -2°). The distribution of the x-component of the external velocity on these two wings is illustrated in Figs. 3 and 4. This indicates that streamwise instabilities will be the most significant ones at low freestream velocities, but crossflow disturbances may come to dominate at higher velocities.

The main conclusion of Ref. (11) was that non-parallel effets are negligible on streamwise instabilities, but can be quite significant on mixed streamwise/crossflow disturbances and indeed very strong on purely crossflow ones. One very interesting observation that was made concerned the influence of the non-parallel effects on the critical wave orientation and frequency. It was found that including the non-parallel effects could result in the dominant instability shifting from a streamwise to a crossflow one, and produce a decrease of the critical frequency, which

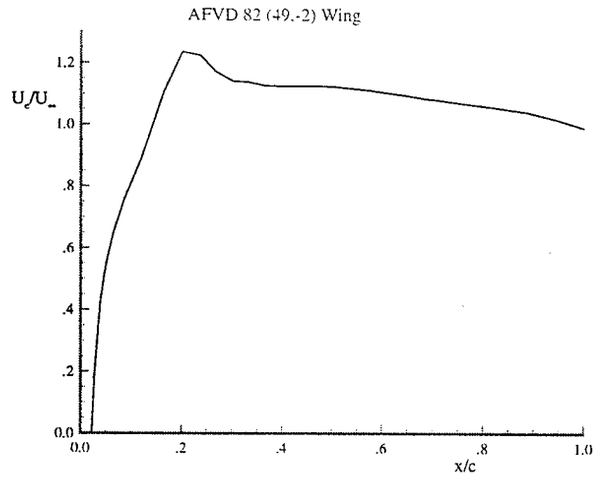

Figure 4: AFVD 82 (49,-2) — External velocity distribution

otherwise is not affected by the non-parallel effects. This behaviour was linked to the presence of two maxima in the fluctuation spectrum, a feature observed experimentally[12], but not predicted by the parallel stability equations.

In this section, we will compare our predictions with hot-wire and hot-film measurements[12]. For the PSE results, we will therefore use the amplitudes based on the u-component of perturbation velocity at a fixed position with respect to the wall and the shear stress at the wall, denoted $\hat{A}_{u_y}$ and $\hat{A}_\tau$ respectively (see Section 2.3). The energy amplitude, $\hat{A}_e$, will also be used to illustrate the influence of the amplitude selection. This possibility of selecting the amplitude does not exist with the OS theory, which should give the PSE an advantage when comparisons are made with experimental results.

This comparison with experimental results will be done in the form of fluctuation spectra at a fixed position x_s. The experimental spectra represent the frequency distribution of the perturbation amplitude. Numerically, the spectral distributions of amplitude are obtained from the n factor as:

$$A_m(f, x_s) = A_{m_0} e^{n_m(f,x_s)} \qquad (15)$$

where subscript m indicates the various possible choices for the PSE amplitude, as in Eq. (7). The unknown initial amplitude A_{m_0} is determined by matching the peaks in the numerical and experimental spectra at the most downstream location. It is assumed that the initial amplitude is the same for all frequencies.

We first present results for the AFVD 82 wing for which hot-film measurements are available[12]. Non-parallel results have already be presented in Ref. (13) for three freestrean velocities, namely 28, 38, and 42.5 m/s. We now examine as well the parallel results for the two extreme velocities. Figures 5 and 6 are comparisons between the experimental data and the predicted spectra at two locations on the wing for the case of the lower freestream velocity. In this case, A_{m_0} has been determined by matching the numerical and experimental maxima at $x_s/c = 0.35$, as shown on Fig. 6. The predicted non-parallel spectra based on the shear stress, $A_\tau^{\mathrm{PSE}}(f, x_s)$, are in very good qualitative and good quantitative agreements with the experimental data over a wide range of frequencies. Departures between $A_\tau^{\mathrm{PSE}}(f, x_s)$ and the measured amplitude are only noted at very low frequencies where the experimental data are not expected to be reliable. The PSE results are in better agreement with the experimental data than the parallel ones, denoted by $A^{\mathrm{OS}}(f, x_s)$, in terms of amplitude levels as well as peak frequency and overall behaviour.

Figures 8-9 present similar comparisons for the same wing operating at $Q_\infty = 42.5$ m/s. A_{m_0} has been calculated at $x_s/c = 0.35$. Behaviours similar to those of the lower freestream velocity case are observed, confirming our findings. The PSE results based on the energy amplitude are also shown on these figures. It is interesting to note that the behaviour of $A_e^{\mathrm{PSE}}(f, x_s)$ is very similar to that of $A^{\mathrm{OS}}(f, x_s)$, especially at the two upstream stations. This might be related to the fact that the energy amplitude, resulting from an integration through the boundary layer thickness, is less sensitive to local features of the flow, as is the Orr-Sommerfeld approach.

Figures 10 to 13 show the parallel and non-parallel results obtained on the ONERA D wing at $Q_\infty = 75$ m/s, along with hot-wire measurements[12]. The trends observed on the AFVD 82 wing can also be seen on the ONERA D wing. However, the improvement in accuracy obtained by using the PSE approach instead of the parallel formulation is much less significant in this case.

5 Conclusion

The Parabolised Stability Equations (PSE) provide a natural framework for the inclusion of non-parallel effects in stability analysis. This article described the mathematical formulation of the PSE as well as their numerical implementation. In the PSE approach, the amplitude of a perturbation can be related to a "physically measurable" quantity, a possibility that does not exist with the parallel stability theory. This feature was demonstrated to be physically relevant, the numerical spectra obtained with the PSE and an amplitude corresponding to the quantity experimentally measured being in better agreement with the experimental ones than those resulting from parallel (Orr-Sommerfeld) calculations.

Acknowledgements

This work was supported in part by a NSERC R&D Grant, in collaboration with the Bombardier Aerospace Group. M. Langlois and P. MacDonald wish to acknowledge the support of FCAR and NSERC, respectively, in the form of Graduate Scholarships. The support of NSERC and FCAR in the form of research grants to C. Masson is gratefully acknowledged.

References

(1) H.L. Reed, W.S. Saric, and D. Arnal. Linear Stability Theory applied to Boundary Layers. *Annual Review of Fluid Mechanics*, 28:389–428, 1996.

(2) M. Gaster. On the effects of boundary-layer growth on flow stability. *Journal of Fluid Mechanics*, 66(3):465–480, 1974.

(3) W.S. Saric and A.H. Nayfeh. Nonparallel stability of boundary-layer flows. *Physics of Fluids*, 18(8):945–950, 1975.

(4) T. Herbert and F.P. Bertolotti. Stability Analysis of Nonparallel Boundary Layers. *Bull. Am. Phys. Soc.*, 32, 1987.

(5) M. Simen, F.P. Bertolotti, S. Hein, A. Hannifi, D. Henningson, and U. Dallmann. Nonlocal and Nonlinear Instability Theory. In John Wiley & Sons Ltd., editor, *Computational Fluid Dynamics '94*, pages 169–179, 1994.

(6) J.A. Masad and M.R. Malik. Effects of body curvature and nonparallelism on the stability of flow over a swept cylinder. *Physics of Fluids*, 6(7):2363–2379, 1994.

(7) C. Masson, S. Boivin, M. Langlois, and I. Paraschivoiu. Curvature and Nonparallel Effects in 3-D Compressible Transition Analysis. AIAA Paper 97-0824, 1997.

(8) C. Masson, R. Martinuzzi, M. Langlois, I. Paraschivoiu, and F. Tezok. Transition Prediction Capabilities for Conical Wings in the Transonic Regime. *Canadian Aeronautics and Space Journal*, 41(1):28–39, 1995.

(9) C. Masson, M. Langlois, and I. Paraschivoiu. Influence of Spanwise Pressure Gradients on Transition Prediction in Transonic Flows. In *Nonlinear Instability and Transition in Three-Dimensional Boundary-Layers*, pages 157–166, Manchester, 1995. IUTAM.

(10) M. Langlois, G. Casalis, and D. Arnal. On the Practical Application of the PSE Approach to Linear Stability Analysis. *Aerospace Science and Technology*, 1997. Article accepted for publication.

(11) M. Langlois, G. Casalis, C. Masson, and I. Paraschivoiu. Non-Parallel Effects in Stability Analysis by the PSE Approach. In *Proceedings of the CASI 6th Aerodynamics Symposium*, pages 45–55, Toronto, 1997.

(12) D. Arnal and J.C. Juillen. Three-Dimensional Transition Studies at ONERA/CERT. AIAA Paper 87-1335, 1987.

(13) M. Langlois, P. MacDonald, G. Casalis, C. Masson, and I. Paraschivoiu. A Detailed Comparison of Non-Parallel Stability Results with Experimental Data. AIAA Paper 98-0335, 1998.

(14) G. Casalis. Transition de la couche limite — Extension de l'approche PSE aux écoulements tridimensionnels. Technical Report DERAT no. 89/5118.03, ONERA/CERT, 1994.

(15) C. Airiau. *Stabilité linéaire et faiblement non linéaire d'une couche limite laminaire incompressible par un système d'équations parabolisé (PSE).* PhD thesis, ENSAE, Toulouse, 1994.

(16) D. Arnal. Boundary Layer Transition: Predictions based on Linear Theory. In *AGARD AR-793*, 1993.

(17) M.R. Malik, S. Chuang, and M.Y. Hussaini. Accurate numerical solution of compressible, linear stability equations. *Journal of Applied Mathematics and Physics*, 33:189–201, 1982.

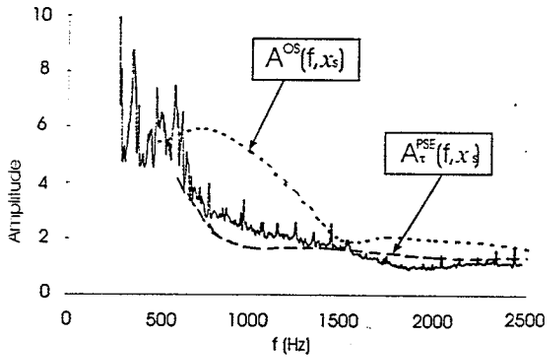

Figure 5: AFVD 82 (49,-2) — Fluctuation spectrum, Q_∞=28 m/s, x_s/c=0.25

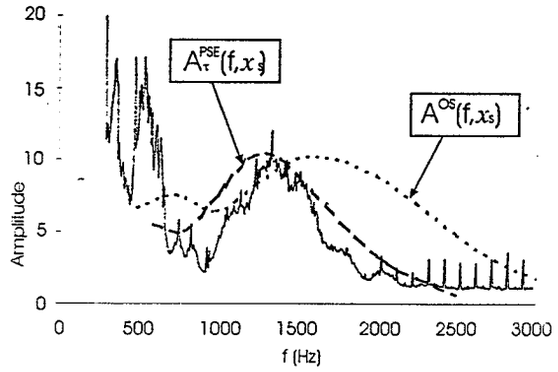

Figure 6: AFVD 82 (49,-2) — Fluctuation spectrum, Q_∞=28 m/s, x_s/c=0.35

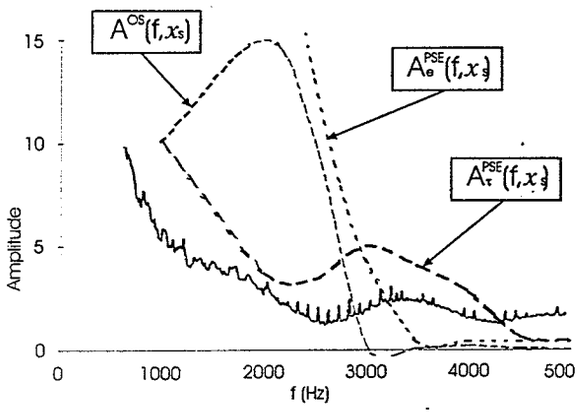

Figure 7: AFVD 82 (49,-2) — Fluctuation spectrum, Q_∞=42.5 m/s, x_s/c=0.25

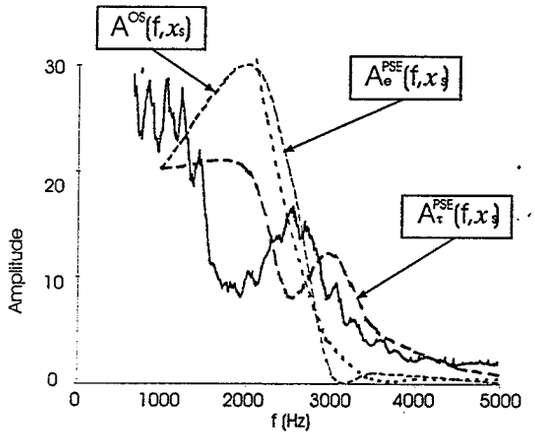

Figure 8: AFVD 82 (49,-2) — Fluctuation spectrum, Q_∞=42.5 m/s, x_s/c=0.30

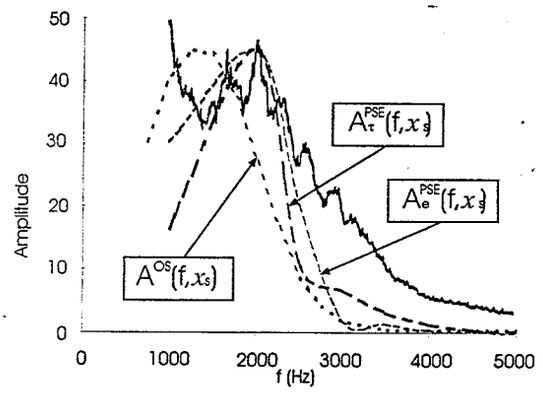

Figure 9: AFVD 82 (49,-2) — Fluctuation spectrum, Q_∞=42.5 m/s, x_s/c=0.35

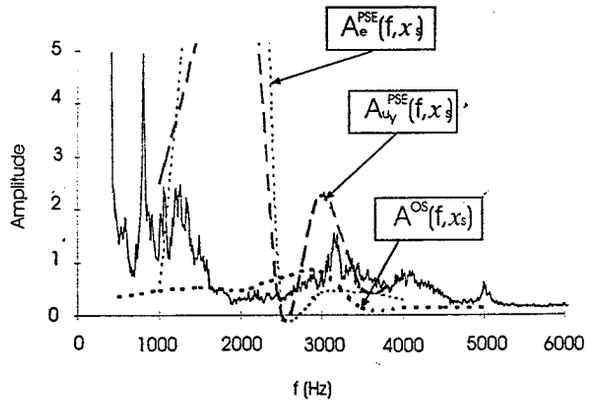

Figure 10: ONERA D (60,-4) — Fluctuation spectrum, Q_∞=75 m/s, x_s/c=0.25

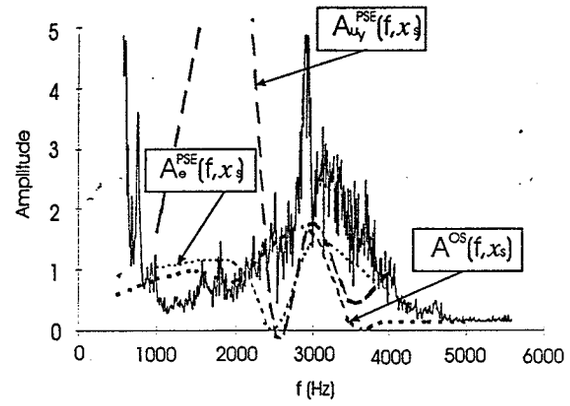

Figure 11: ONERA D (60,-4) — Fluctuation spectrum, Q_∞=75 m/s, x_s/c=0.30

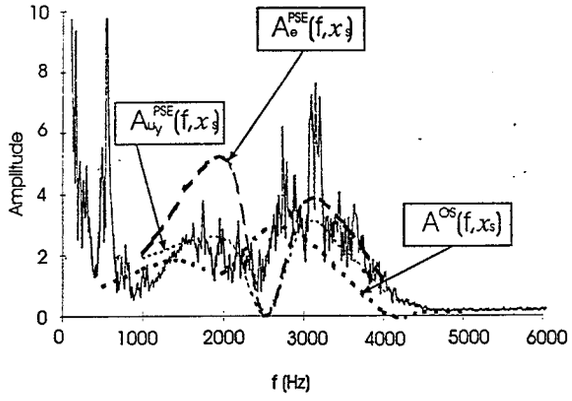

Figure 12: ONERA D (60,-4) — Fluctuation spectrum, Q_∞=75 m/s, x_s/c=0.35

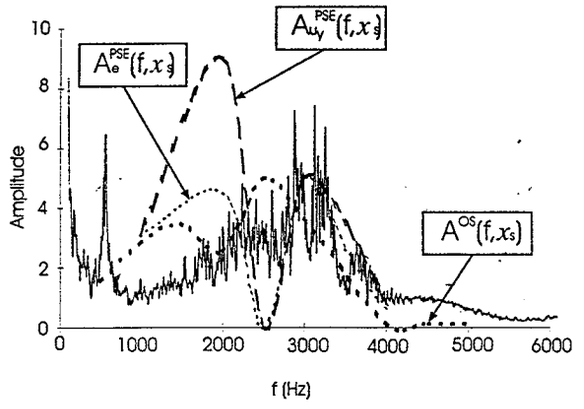

Figure 13: ONERA D (60,-4) — Fluctuation spectrum, Q_∞=75 m/s, x_s/c=0.40